RSC Advances

PAPER

View Article Online
View Journal | View Issue

Check for updates

Cite this: *RSC Adv.*, 2020, **10**, 33534

Sophora interrupta Bedd. root-derived flavonoids as prominent antiviral agents against Newcastle disease virus†

Cherukupalle Bhuvaneswar,[ad] Aluru Rammohan, *[be] Baki Vijaya Bhaskar,[g] Pappithi Ramesh Babu,[a] Gujjar Naveen,[c] Duvvuru Gunasekar,[b] Subbiah Madhuri, *[c] Pallu Reddanna[f] and Wudayagiri Rajendra *[a]

The discovery and development of novel antiviral drugs from natural sources is continuously increasing due to limitations of currently available drugs such as toxic side effects, drug residue risk factors, high costs, and poor therapeutic strategies. Also, there are very few known antiviral drugs that are effective against only specific viruses. Hence, the present study is intended to isolate and characterize potent antiviral compounds from the methanolic root extract of *Sophora interrupta* Bedd. against avian paramyxovirus, Newcastle disease virus (NDV) and to distinguish the molecular basis of antiviral compounds. The two isolated flavonoids, maackiain (**SR-1**) and echinoisoflavanone (**SR-2**) exhibited the best antiviral activities against NDV infection in chicken embryo fibroblast cell lines compared to the standard antiviral drug, Ribavirin. Further, the *in vitro* studies and quantitative PCR analysis suggests that these flavonoids inhibit the viral entry, replication, and transcription, which may be beneficial as a promising strategy for the treatment of viral infections. Besides, the molecular docking studies of **SR-1** and **SR-2** exhibited high binding affinities of −7.6 and −8.0 kcal mol^{-1}, respectively, and marked interactions with the NDV surface glycoprotein, hemagglutinin neuraminidase (HN). Also, the *in silico* toxicity properties as well pharmacokinetic studies of isolates revealed them as pharmacologically potent antiviral compounds.

Received 26th February 2020
Accepted 3rd June 2020

DOI: 10.1039/d0ra01820a

rsc.li/rsc-advances

Open Access Article. Published on 10 September 2020. Downloaded on 1/17/2026 8:55:58 AM.
This article is licensed under a Creative Commons Attribution-NonCommercial 3.0 Unported Licence.

1. Introduction

Among all the poultry diseases, influenza (HPAI) and Newcastle disease (ND) are the two foremost diseases that have caused economically devastating results in poultry farms, which in turn affects the human health due to malnutrition.[1,2] NDV can infect more than 250 bird species across the world.[3] The onset of Newcastle disease is rapid and clinical signs involving respiratory, digestive, and/or nervous systems appear within 48 h. The severity of this disease (high morbidity and mortality) depends on the infecting strain and the bird's susceptibility.[3] The currently used vaccines are not 100% protective and disease outbreaks have been recorded in vaccinated flocks. On the other hand, antiviral drugs are not ideal due to their side effects, expensive treatment procedures, and moreover, the fear of accumulation of residues in meat and/or eggs. For example, Ribavirin a well-known broad-spectrum antiviral drug against various RNA viruses[4–6] and approved for the treatment of respiratory syncytial virus (RSV) frequently results in lower respiratory tract infections in children. However, there are some concerns about its efficacy due to its potential toxic effects on the exposed individuals when administered *via* aerosol and the high price of the drug.[7,8] All these factors reiterate the necessity for the identification of novel antiviral drugs from natural sources.[9,10] Although a few plant extracts have shown good anti-NDV activity,[11] none of them are in commercial use. It may be due to insufficient work in the area of the active component(s) identification, which is accountable for the antiviral activities and their mechanism of action. Hence, it is essential to identify and characterize bioactive component(s) from natural sources that could display promising antiviral activities.

Plants are a rich source of new and novel natural compounds[12–14] for the development of active pharmaceutical ingredients. *Sophora interrupta* Bedd. belongs to the family Fabaceae, which is an endemic medicinal plant of Tirumala Tirupati hill ranges of Chittoor district, Andhra Pradesh,

[a]*Department of Zoology, Sri Venkateswara University, Tirupati-517502, AP, India. E-mail: rajendraw2k@yahoo.co.in*
[b]*Natural Products Division, Department of Chemistry, Sri Venkateswara University, Tirupati-517502, AP, India*
[c]*National Institute of Animal Biotechnology (NIAB), Hyderabad-500049, AP, India*
[d]*Department of Microbiology, Sri Venkateswara University, Tirupati-517502, AP, India*
[e]*Department of Organic and Biomolecular Chemistry, Ural Federal University, Yekaterinburg 620002, Russian Federation*
[f]*School of Life Sciences, University of Hyderabad (UOH), Hyderabad-500046, Telangana, India*
[g]*Department of Pathophysiology, Shantou University Medical College, Shantou, Guangdong, China-515031*

† Electronic supplementary information (ESI) available. See DOI: 10.1039/d0ra01820a

This journal is © The Royal Society of Chemistry 2020

Open Access Article. Published on 10 September 2020. Downloaded on 1/17/2026 8:55:58 AM.
This article is licensed under a Creative Commons Attribution-NonCommercial 3.0 Unported Licence.

India.[15] The genus *Sophora* is commonly used in Indian Ayurvedic medicine as well as traditional Chinese medicine as a remedy to cure several diseases and disorders.[16–20] Two flavonoids, anagyrine and sophoranol, were isolated from *Sophora flavescens*, which were found to show antiviral activity against RSV.[21] Earlier reports on *S. interrupta* resulted in few flavonoids, isoflavonoids, coumarins, and other phenolic compounds.[22,23] Besides, our preliminary investigations have revealed that the root extracts of *Sophora interrupta* showed less oxidative stress and lowered the viral titer in NDV-infected chickens.[23] Even though few biomolecules have been isolated from *Sophora interrupta* Bedd., to the best of our knowledge, there is no antiviral report on this endemic plant (except for our preliminary investigations) and hence, it was considered for the current investigations. Therefore, the present work is intended to isolate and characterize the antiviral compounds from the methanolic root extract of *Sophora interrupta* Bedd. and to evaluate their antiviral activities in order to optimize the lead molecules against Newcastle disease viral infections.

2. Materials and methods

2.1. General experimental procedures

All chemicals and solvents were of analytical grade, were purchased from Merck, India, and used without further purification. HPLC analysis was carried out using a Shimadzu HPLC system equipped with a binary gradient system with a variable UV-Vis-detector (SPD-20A) comprising a Rheodyne injection valve with a loop size of 20 μL, LC-20AD pumps, and an integrator. Thin layer chromatography (TLC) was performed by using silica gel 60 F_{254} pre-coated plates (Merck) and column chromatography was performed on 100–200 mesh size silica gel (0.08 mm thickness, Acme). Melting points were determined using a Kofler hot stage apparatus and are uncorrected. The ESI-TOF-MS spectra were recorded in the positive mode on an API Q-STAR PULSA I spectrometer of Applied Biosystems. UV spectra were measured in MeOH on a Shimadzu UV-1800 spectrophotometer. The IR spectra were recorded using a Bruker Alpha-Eco ATR-FTIR spectrophotometer, and the ^{1}H and ^{13}C NMR spectra were recorded on a Bruker Avance spectrometer operating at 600 MHz for ^{1}H and 150 MHz for ^{13}C, using DMSO-d_6 with TMS as the internal standard.

2.2. Collection of the plant material

The roots of *Sophora interrupta* Bedd. were collected from Kumaradhara Theertham of the Tirumala-Tirupati hill ranges, Chittoor district, AP, India. The plant species was identified and authenticated by Dr K. Madhava Chetty, Plant Taxonomist, Department of Botany, Sri Venkateswara University, Tirupati, India, wherein a voucher specimen (No. 721) was deposited.

2.3. Extraction of the plant material

Solvent extraction was carried out by the method described by Parekh and Chanda[24] with slight modifications. 500 g of shade-dried and powdered roots of *Sophora interrupta* was soaked in MeOH in the 1 : 5 ratio (w/v) in conical flasks plugged with aluminum foils. After proper soaking for 48 h, the solvent was collected and re-extracted thrice, and the supernatant solvents were pooled and filtered using Whatman No. 1 filter paper after treating with charcoal powder. The combined methanol extracts were concentrated under reduced pressure using a Büchi rotary evaporator. The solvent-free extract was stored at 4 °C in air tight bottles for further study.

2.4. Isolation of the flavonoids

The concentrated methanol extract (25 g) was refluxed with *n*-hexane to remove oils and fats, and the *n*-hexane insoluble portion was eluted with ethyl acetate. Further, the ethyl acetate soluble fraction (13 g) was separated over a silica gel (100–200 mesh) column using *n*-hexane–ethyl acetate step gradient solvent system. The *n*-hexane–ethyl acetate eluents, with concentrations in the ratio of 7 : 3 and 6 : 4, were employed for the concentration of the separated fractions, followed by crystallization, which yielded colorless prisms (**SR-1**, 43 mg) and a yellow crystalline solid (**SR-2**, 47 mg), respectively (Fig. 1).

2.4.1. 3-Hydroxy-8,9-methylenedioxypterocarpan or maackiain (SR-1). **SR-1** was crystallized from CH_2Cl_2 as colorless prism-shaped crystals. Mp: 193–195 °C; UV (MeOH) λ_{max} (log ε): 218 (4.85), 281 (sh) (4.53), 287 (4.62), 310 (4.83) nm; FT-IR (ν_{max}, KBr): 3235 (–OH), 2980, 2956, 2887, 1624 (>C=C<), 1595, 1505, 1472, 1451, 1369, 1336, 1318, 1252 (C–O), 1179, 1140, 1122, 1047, 1030, 941 (–OCH_2O–), 923, 861, 827, 736, 623 cm^{-1}; ^{1}H NMR (600 MHz, DMSO-d_6) δ: 9.62 (1H, s, OH-4), 7.23 (1H, d, J = 8.4 Hz, H-1), 6.95 (1H, s, H-7), 6.51 (1H, s, H-10), 6.45 (1H, dd, J = 8.4, 2.4 Hz, H-2), 6.25 (1H, d, J = 2.4 Hz, H-4), 5.93 (1H, d, J = 1.0, H-12a), 5.90 (1H, d, J = 1.0, H-12b), 5.49 (1H, d, J = 6.8 Hz, H-11a), 4.21 (1H, dd, J = 10.5, 4.3 Hz, H-6_{ax}), 3.59 (1H, dd, J = 10.5, 9.5 Hz, H-6_{eq}), 3.53 (1H, ddd, J = 9.5, 6.8, 4.3 Hz, H-6a); ^{13}C NMR: (150 MHz, DMSO-d_6) δ: 158.7 (C-3), 156.3 (C-4a), 153.7 (C-10a), 147.4 (C-9), 141.0 (C-8), 132.0 (C-1), 118.4 (C-6b), 111.3 (C-11b), 109.7 (C-2), 105.4 (C-7), 102.8 (C-4), 101.0 (C-12), 93.2 (C-10), 78.0 (C-11a), 65.8 (C-6), 39.5 (C-6a); ESI-TOF-MS (m/z): calculated for $C_{16}H_{13}O_5$ $[M + H]^+$ 285.0763, found 285.0775.

2.4.2. 2′,4′-Dimethoxy-3′-(γ,γ-dimethylallyl)-3,5,7-trihydroxy-isoflavanone or echinoisoflavanone (SR-2). **SR-2** was crystallized from MeOH as a yellow crystalline solid, Mp: 198–

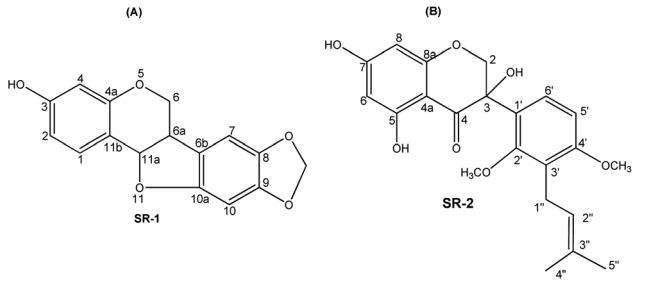

Fig. 1 Structures of the isolated compounds (A) maackiain (**SR-1**) and (B) echinoisoflavanone (**SR-2**) isolated from roots of *Sophora interrupta* Bedd.

Open Access Article. Published on 10 September 2020. Downloaded on 1/17/2026 8:55:58 AM. This article is licensed under a Creative Commons Attribution-NonCommercial 3.0 Unported Licence.

199 °C; UV (MeOH) λ_{max} (log ε): 222 (4.83), 293 (4.97), 338 (sh) (4.36) nm; FT-IR (ν_{max}, KBr): 3476, 3337 (–OH), 2991, 2931, 1616 (>C=O), 1577, 1507, 1485, 1464, 1413, 1373, 1298, 1260, 1211, 1154, 1103, 1081, 1011, 945, 828, 805, 754, 636 cm^{-1}; ^1H NMR: (600 MHz, DMSO-d_6) δ: 12.14 (1H, s, OH-5), 10.80 (1H, s, OH-7), 6.61 (1H, s, OH-3), 7.39 (1H, d, J = 8.6 Hz, H-6′), 6.80 (1H, d, J = 8.6 Hz, H-5′), 5.94 (1H, d, J = 2.1 Hz, H-6), 5.90 (1H, d, J = 2.1 Hz, H-8), 5.12 (1H, brt, J = 6.5 Hz, H-2″), 4.55 (1H, d, J = 11.7 Hz, H-2a), 4.02 (1H, d, J = 11.7 Hz, H-2b), 3.77 (3H, s, OMe-4′), 3.49 (3H, s, OMe-2′), 3.24 (2H, brd, J = 6.5 Hz, CH_2-1″), 1.66 (3H, s, Me-5″), 1.62 (3H, s, Me-4″); ^{13}C NMR: (150 MHz, DMSO-d_6) δ: 195.0 (C-4), 166.6 (C-7), 164.6 (C-5), 162.5 (C-8a), 158.8 (C-4′), 155.5 (C-2′), 131.0 (C-3″), 126.0 (C-6′), 124.2 (C-1′), 122.8 (C-2″), 121.8 (C-3′), 106.0 (C-5′), 100.3 (C-4a), 96.2 (C-6), 94.9 (C-8), 74.2 (C-2), 73.5 (C-3), 61.2 (OMe-2′), 56.8 (OMe-4′), 25.4 (C-4″), 23.5 (C-1″), 17.8 (C-5″); ESI-TOF-MS (m/z): calculated for $C_{22}H_{25}O_7$ $[M + H]^+$ 401.1600, found 401.1602.

2.5. Analyses of the root extract and isolates by HPLC

The methanol extract and the isolated compounds were qualitatively analyzed by High Performance-Liquid Chromatography (HPLC), according to the standard procedure.[25] Reverse phase chromatographic analysis was carried out in isocratic conditions using 0.4% methanol and acetic acid (80 : 20 v/v) as the mobile phase over a C-18 reverse phase column at 25 °C with a flow rate of 1 mL min^{-1}. The compounds were detected at 293 nm wavelength using a UV-Vis detector.

2.6. Cell lines

Chicken fibroblast (DF-1) cells were obtained from American Type Culture Cells (*ATCC-CRL-12203*), USA, and they were revived and sub-cultured in BSL-II laboratory. The DF-1 cells were cryopreserved in a liquid nitrogen tank (−196 °C) for further use. Dulbecco's Modified Eagle Medium (DMEM) was supplemented with 10% Fetal Bovine Serum (FBS), penicillin, and streptomycin were used for routine sub-culturing and for the *in vitro* experiments.

2.7. Cytotoxic assay

The isolated compounds **SR-1** and **SR-2** were tested for their cytotoxic effects on chicken embryo fibroblast cell line (DF-1) by the MTT [3-(4,5-dimethylthiazol-2-ol)-2,5-diphenyltetrazolium bromide] assay, according to the method described by Mosmann[26] with slight modifications. The DF-1 cells were seeded onto 96-well cell culture plates at a density of 1.5×10^4 cells per well in DMEM supplemented with 10% FBS and incubated for 6–8 h to allow the cells to form a monolayer. The cells were incubated with increasing concentrations of isolated compounds (3–500 μg mL^{-1}) in triplicates and allowed to proliferate for 72 h at 37 °C in 5% CO_2. The culture medium was discarded and the cells were subsequently washed with phosphate-buffered saline (PBS) thrice. 20 μL of the MTT reagent at a concentration of 5 mg mL^{-1} was added to each well for the development of formazan. Further, 100 μL of MTT-solubilizing solution was added to each well of the plates and the plates were incubated at 37 °C in 5% CO_2 for 1 h to solubilize the formazan crystals. The absorbance was measured at 570 nm using a multi-mode plate reader. The cytotoxicity of the compounds was expressed as CC_{50} and Maximum Non-Toxic Concentration (MNTC), which is the safest concentration at which 100% cells are viable. Thus, the percentage of cell viability was calculated at this concentration.

2.7.1. Viral plaque assay. Viral plaque assay was performed to investigate and quantify the infectivity of NDV (mesogenic strain Komarov) in the DF-1 cells. A 24-well plate was seeded with 1.5×10^5 DF-1 cells and incubated overnight at 37 °C in 5% CO_2. The cells were then infected with 100 μL of ten-fold serial dilutions (10^{-1} to 10^{-7}) of NDV and incubated at 37 °C with occasional shaking for 1 h. After an hour of virus adsorption, the cells were washed with PBS and overlaid with DMEM in 1% FBS containing 0.8% methylcellulose. The infected cells were incubated at 37 °C in 5% CO_2 for 5 days until the development of plaques. The cells were fixed with methanol (1 mL per well) for 15 min and stained with 0.3 mL per well of 1% crystal violet for 30 min, and the strain was washed off with distilled water. The plates were then dried at 37 °C and the number of plaques for each virus dilution was counted. The plaque forming units (PFU) were thus calculated.

2.7.2. Plaque reduction assay. The inhibitory effect of the compounds on NDV infection was investigated by plaque reduction assay. The antiviral activity was evaluated by treating the DF-1 cells with the pre-addition, post-addition, and simultaneous addition of different concentrations of the compounds (10, 20, 30, and 40 μg mL^{-1}) during NDV infection and compared with Ribavirin as the standard control drug. The compounds were diluted in 1% DMSO with DMEM. The titer and dilutions of the virus used for this assay were 2^9 HAU and 10^{-5} μL, respectively, and the volume of virus added was 100 μL per well (50 plaques per well based on the viral plaque assay, 50×10^4 PFU mL^{-1}).

2.8. Quantification of viral RNAs

2.8.1. Construction of plasmid NP for real-time PCR assay. Amplified NDV NP gene was used for the construction of NP plasmid, followed by the quantification of viral RNAs, according to the method of Qiu *et al.*[27] Specific primers were designated for the NDV-NP gene of gRNA, cRNA, and mRNA using the gene runner software, based on the NP gene ORF sequence of the Komarov strain of NDV. The sequence of the NP gene was obtained from Genbank (Id # KT445901.1). The primers for the NP gene of gRNA, cRNA, and mRNA were identified, and the designed primers displayed stable and specific amplification efficiency.

2.8.1.1. Viral RNA isolation and NP gene amplification. RNA was extracted from the allantoic fluid of NDV-infected eggs by Trizol reagent. The concentration and purity of the isolated RNA were determined by a NanoDrop UV-Vis spectrophotometer. Genomic RNA was reverse transcribed by a random hexamer primer (TAKARA) following the manufacturer's instructions and the resulting cDNA fragments were subjected to PCR for amplification. PCR was set up with 50 μL reaction mixture using 2.5 U *Taq Polymerase*, 5 μL of 10 × PCR buffer (Mg^{2+}), 8 μL

 This journal is © The Royal Society of Chemistry 2020

Open Access Article. Published on 10 September 2020. Downloaded on 1/17/2026 8:55:58 AM.
This article is licensed under a Creative Commons Attribution-NonCommercial 3.0 Unported Licence.

2.5 mM dNTP mixture, 5 μL of cDNA fragments, 1 μL of 20 μM forward primer for the NP gene (FPNP), and 1 μL of 20 μM reverse primer for the NP gene (RPNP) for the amplification of the NP gene. The PCR cycle conditions were 95 °C for 1 min, 25 cycles of 94 °C for 30 s, 55 °C for 30 s, and 72 °C for 90 s, followed by 72 °C for 10 min. 50 μL PCR amplicons were electrophoresed in 1.5% agarose gel stained with ethidium bromide in the presence of 10 μL of the gel loading buffer. Electrophoresis was carried out at 70 V for 50 min. The gel containing band was carefully cut and weighed, followed by extraction according to the Nucleospin DNA purification kit. After determining the purity, the NP gene was subjected to cloning.

2.8.1.2. Cloning and transformation. Competent cells ($DH5^{\alpha}$ cells) were prepared and the purified PCR product was subcloned into a TOPO vector to construct a plasmid. TA cloning was performed to insert the gene of interest (NP gene) into the TOPO vector. This ligation mixture (plasmid) was transformed to competent cells and streaked on Luria Agar plates. The colonies were isolated and subjected to PCR, as described above for the confirmation of gene insertion into the plasmid. The positive colonies were grown in Luria broth for propagation.

2.8.1.3. Plasmid isolation and conformation of the NP gene. Plasmid DNA was isolated from the colonies and purified by using QIAGEN plasmid midi kit. The concentration and purity of the plasmid were determined by an ND 1000 spectrophotometer (NanoDrop Technologies, Inc.). The purified plasmid was subjected to restriction digestion with ECORI and run on agarose gel for the confirmation of the NP gene.

2.8.2. Viral infections and treatment. DF-1 cells were seeded onto 6-well plates at a density of 6×10^5 cells per well and incubated at 37 °C in 5% CO_2 for 2 h, followed by washing with PB. The isolated compounds **SR-1**, **SR-2**, and the standard RB at below their MNTC (Maximum Non-Toxic Concentration), *i.e.*, 40 μg mL^{-1} at a volume 400 μL per well were added separately to the cells. After incubating for 2 h at 37 °C in 5% CO_2, the compound solution was removed, the cells were carefully washed twice with PBS, and were incubated with DMEM supplemented with 1% FBS at 37 °C in 5% CO_2 for 2 days.

2.8.2.1. Viral RNA extraction. The total RNA of the virus was extracted from the virus-infected cells according to the manufacturer's protocol using Trizol reagent. Cellular DNA was degraded by the addition of *DNase I* to the samples at a final concentration of 1 U μL^{-1} at 37 °C for 40 min and then inactivated at 65 °C for 10 min in the presence of 5 mM EDTA. These purified RNA samples were subjected to reverse transcription PCR using gRNA, cRNA, and mRNA-NP gene-specific reverse transcription primers.

2.8.2.2. Standard specific reverse transcription PCR by GSP (Pla-G, Pla-R, Pla-18T for gRNA, cRNA, and mRNA). Strand-specific reverse transcription of NDV gRNA (viral genomic RNA), cRNA (complementary RNA), and mRNA (messenger RNA) was performed with specially designed reverse transcription primer sets. To quantify the three kinds of cDNAs, each with one pair of primers, reverse transcription primers specific to gRNA, cRNA, and mRNA were designed using the Gene Runner software. 10 μL of each RNA sample was reverse transcribed by respective primers in the presence of reverse transcriptase (TAKARA), according to the manufacturer's instructions. Each reaction mixture contained 10 μL of each RNA sample, 200 U reverse transcriptase, 5 μL 5 × RT buffer, 10 mM specific RT primer, 10 mM dNTPs, and ultrapure water in a final volume of 25 μL. The mixture was incubated at 42 °C for 60 min and then at 75 °C for 15 min. The DNA fragments were precipitated using ethanol. Finally, the pellet was dissolved in 20 μL ultra-pure water and stored at −80 °C for further use. The resulting reverse transcripts (cDNAs) specific to gRNA, cRNA, and mRNA were used as templates for Real-Time PCR.

2.8.3. Quantitative real-time PCR. The primers were designed for Real-time PCR according to the "MIQE guidelines for PCR" based on the cDNA sequence of NDV NP gene of Komarov strain in order to obtain suitable NP gene amplification of three kinds of viral cDNAs (from gRNA, cRNA, and mRNA). Quantitative PCR (qPCR) assay was performed using Maxima SYBR Green dye (Life Technologies) and the reverse transcription products, *i.e.*, cDNAs (specific to gRNA, cRNA, and mRNA), as templates. The real-time PCR reaction mixture consists of 5 μL of SYBR Green master mix, 1 μL of reverse transcription product, 25 pmol of each of the forward and reverse primers made up to a final volume of 10 μL with ultrapure water (Gibco BRL). The cycle conditions for qPCR were 95 °C for 5 min, followed by 40 cycles of 95 °C for 15 s, 60 °C for 30 s, and 72 °C for 30 s. Nuclease-free ultrapure water was used as the template for the negative control. The specificity of the primers was monitored by the melting curve analysis and a standard curve was constructed for the linear correlation between the C_q values and the molecular number of cDNA targets by using the NP plasmid.

2.9. Statistical analysis

All the experiments were carried out in triplicate and calculated using SPSS v16. The data was expressed as mean ± standard error of the mean (SEM) and analyzed by one-way analysis of variance (ANOVA), followed by student's "t" test and the findings were considered to be statistically significant if p-value is <0.05.

2.10. *In silico* studies

2.10.1. Protein preparation. Crystal structure hemagglutinin neuraminidase (HN, PDBID: 1USX) protein was retrieved from Protein Data Bank;[28] water molecules, cofactors, and bound ligands were extracted. Energy minimization was employed with the Molecular Operating Environment (MOE) using the following standard parameters and methods such as the addition of hydrogen and the fixing of the gradient to 0.00001; force field MMFF94× was set up with the cut off value from 8 to 10; solvation was set at distance mode; the exterior was set to 8, dielectric was set to 1, and partial charge was fixed for the required calculations. Moreover, these energy-minimized protein targets were used for further studies.

2.10.2. Ligand preparation. The 3D atomic coordinates of the isolates **SR-1** and **SR-2** were successfully retrieved from PubChem. Further, the small molecules were employed for 3D optimization, hydrogen was added, and the energy

Open Access Article. Published on 10 September 2020. Downloaded on 1/17/2026 8:55:58 AM.
This article is licensed under a Creative Commons Attribution-NonCommercial 3.0 Unported Licence.

minimization was performed with an MMFF94× force field. The refined and energy-minimized small molecules were used for the docking experiments. ADME and Lipinski's rule were computed using Molsoft molecular property prediction and Osiris server programs.

2.10.3. Molecular docking. Molecular docking studies were carried out using Auto Dock Vina 4.0 with PyRx interface.[29] Initially, all the ligand molecules were uploaded and energy-minimized with Universal Force Field (UFF) using conjugate-gradient algorithm with 200 run interactions. The docking parameters were set as follows: Lamarckian genetic algorithm was used for the docking program[30] and the number of individuals in the population was set to 150; the maximum number of generations was 27 000 and the number of evaluations was 25 000; the top individuals to survive to the next-generation was set to 1; Gene mutation rate was static at 0.02 and the crossover rate was fixed at 0.8, Cauchy beta was 1.0, and the genetic algorithm window size was set to 10.0. The grid was set to an appropriate binding pocket size and the exhaustiveness was set to 8. The best-docked ligand conformations were saved and the bond lengths, bond angles, and bonding interactions were analyzed using PyMOL.[31]

3. Results and discussion

3.1. Isolation and characterization of flavonoids

The methanol extract of the roots of *Sophora interrupta* was prepared using the standard protocol and concentrated under reduced pressure, which yielded a dark brown gummy solid. To testify the active compound profile of the methanol extract, it was subjected to Reversed-phase High Performance Liquid Chromatography (RP-HPLC) analysis and the crude extracts showed five major peaks with retention times at 2.14, 2.85, 4.92, 5.74, and 8.87 min (Fig. 2A). Further, the methanol extract was subjected to purification over a silica gel column, which yielded two compounds that were designated as **SR-1** and **SR-2**. Thus, the successfully isolated purity of the two compounds was analysed by using HPLC with retention time of 5.0 and 8.8 min, and compared[25,32] with the crude extract profile (Fig. 2B and C). The chemical structures of the isolates (Fig. 1) were established by using UV, FT-IR, ^{1}H NMR, ^{13}C NMR, and ESI-TOF- mass spectral analysis and were characterized as 3-hydroxy-8,9-methylenedioxy-pterocarpan (**SR-1**) and 2′,4′-dimethoxy-3′-(γ,γ-dimethylallyl)3,5,7-trihydroxy-isoflavanone (**SR-2**) as their spectral data were in good agreement with the literature values.[33,34]

3.2. Cytotoxicity assay

Subsequently, the cytotoxicity profiles of **SR-1**, **SR-2**, and the standard drug Ribavirin were determined in chicken embryo fibroblast DF-1 cell lines by the MTT assay.[26] The maximum non-cytotoxic concentration (MNCC), at which no significant changes were detected in the cellular morphology of the DF-1 cells of **SR-1** and **SR-2**, was found to be 62.5 and 40 μg mL^{-1}, respectively, while that of Ribavirin was 31.25 μg mL^{-1}. This suggested that both the compounds are comparatively less toxic than Ribavirin. Based on the results of the MTT assay, the 50% cytotoxic concentration (CC_{50}: the dose that inhibited the growth by 50% compared to the untreated cells) of **SR-1** was determined as 600 μg mL^{-1}, while that for both **SR-2** and Ribavirin was 400 μg mL^{-1}.

3.3. Viral plaque assay and plaque reduction assay

Further, the viral plaque assay was performed to evaluate the antiviral effect of the isolated compounds **SR-1** and **SR-2**, and compared with that of the standard Ribavirin in DF-1 cells. The isolates and Ribavirin with different concentrations such as 10, 20, 30, and 40 μg mL^{-1} were used before, after, and during the NDV infection in order to categorize the stage of the viral life cycle that was probably inhibited.[35,36] The percentage of plaque

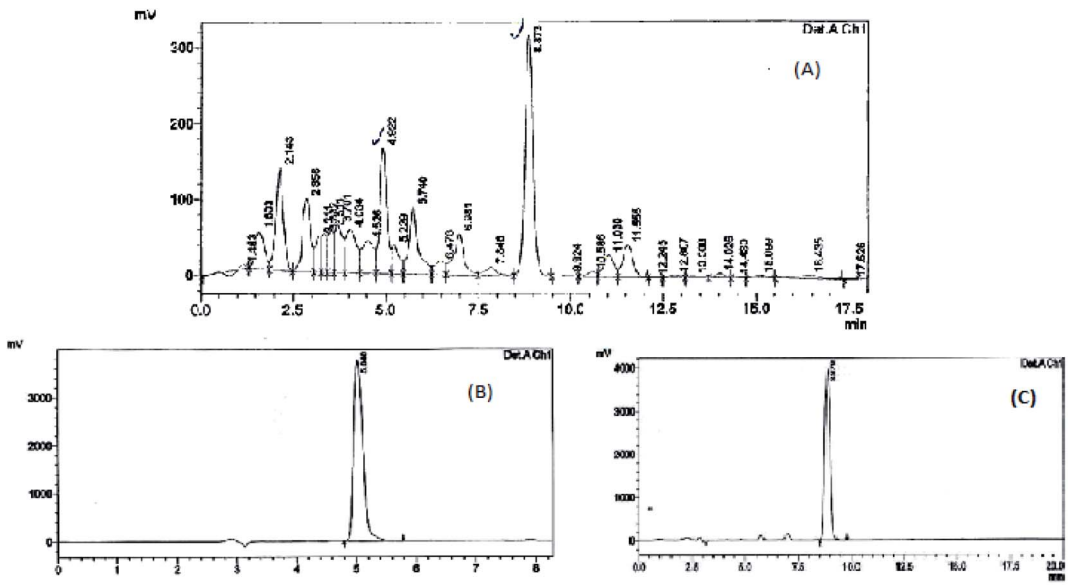

Fig. 2 HPLC chromatograms of (A) the root extract of *Sophora interrupta* Bedd. resolving three major peaks at the retention times of 2.1, 4.9, and 8.8 min; (B) pure compound SR-1 and (C) pure compound SR-2 resolved at the retention time of 5.0 and 8.8 min, respectively.

 This journal is © The Royal Society of Chemistry 2020

Open Access Article. Published on 10 September 2020. Downloaded on 1/17/2026 8:55:58 AM.
This article is licensed under a Creative Commons Attribution-NonCommercial 3.0 Unported Licence.

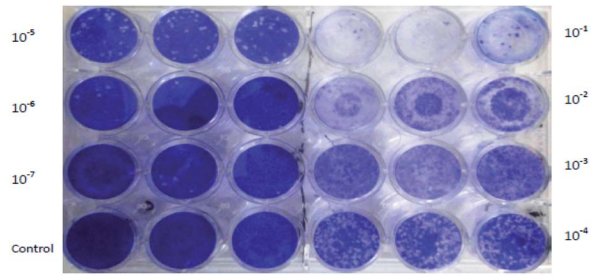

Fig. 3 Viral plaque assay at 10^{-5} dilution of the stock NDV showed 50 plaques and this dilution were was used for all the viral plaque assays.

reduction was determined by calculating the reduction in the number of plaques during compound treatment and compared to the untreated NDV infected cells, which were defined as 100%. Concisely, DF-1 cells (1.5×10^5 cells per well of a 24-well plate) were infected with 10-fold serial dilutions of NDV laboratory stock (2^9 hemagglutination units), followed by overlaying with Dulbecco's Modified Eagle's Medium containing 0.8% methylcellulose without serum supplementation and incubated at 37 °C in 5% CO_2 incubator. After 4 days, the cells were fixed and stained with 1% crystal violet to visualize the viral plaques. At 10^{-5} μL dilution of the stock virus, 50 plaques were observed and this viral dilution was subsequently used as the standard viral infection dose for the entire study (Fig. 3).

To determine whether the test compounds inhibit virus adsorption, DF-1 cells were treated with the compounds for an hour prior to NDV infection. There was a significant reduction in the plaque numbers in the treated cells compared to the untreated controls. The inhibitory concentration (IC_{50}) of **SR-1**, **SR-2**, and Ribavirin was 10, 20, and 40 μg mL^{-1}, respectively. **SR-1** and **SR-2** exhibited strong antiviral activity by decreasing the viral plaques by 67% and 59%, respectively, at their maximum test dose, compared to only 32% viral plaque reduction by Ribavirin at MNCC (Fig. 4A). The results suggest that both **SR-1** and **SR-2** can significantly inhibit viral adsorption and thereby prevent NDV infection at a lesser dose (higher therapeutic index) compared to Ribavirin. In the second assay, the compounds were added to the NDV-infected cells 1 h post-infection. Both IC_{50} and the therapeutic index (TI) values could not be determined at the test doses. A moderate reduction in the viral plaque number was observed compared to the previous experiment; **SR-1** and **SR-2** showed 38% and 35% of viral plaque reduction at their maximum test dose (40 μg mL^{-1}), respectively, compared to only 18% by Ribavirin at MNCC (Maximum Non-Cytotoxic Concentration of 31.25 μg mL^{-1}) (Fig. 4B). The results indicated that the compounds probably interfered with the viral replication and/or transcription, similar to Ribavirin,[37] and further reiterated that the compounds could be better than Ribavirin with respect to the inhibition of NDV infection *in vitro*.

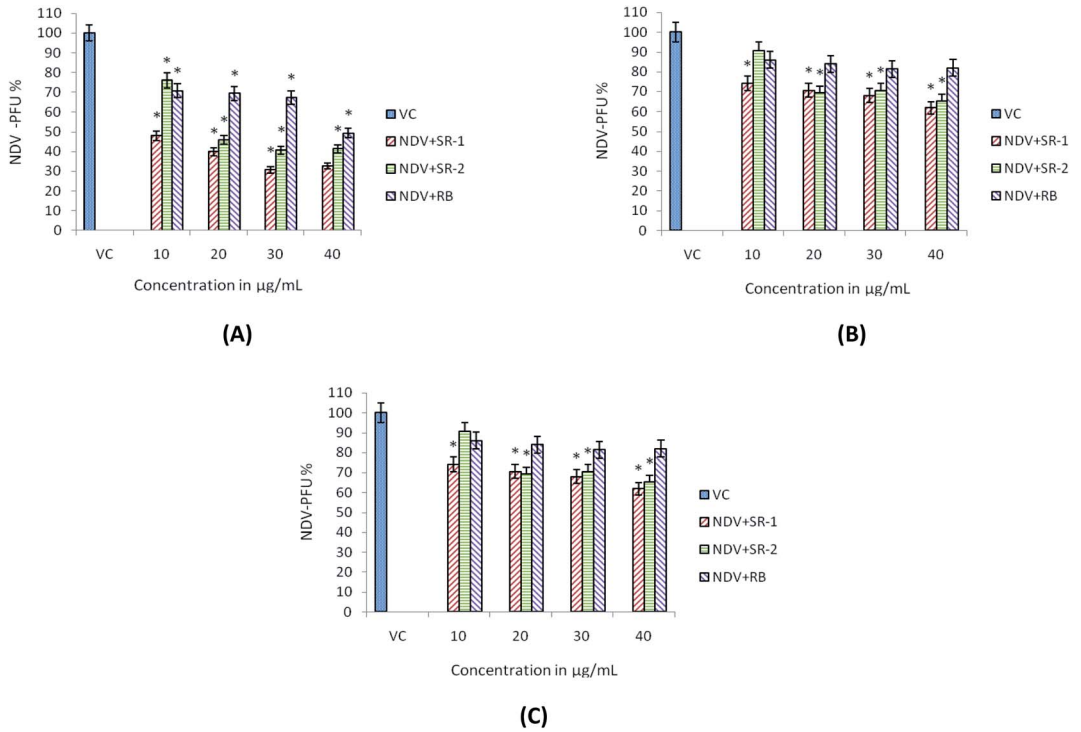

Fig. 4 The investigation of compounds, **SR-1**, **SR-2**, and Ribavirin (RB) on ND virus infection in DF-1 cells treated at different concentrations: (A) pre-treatment of the cells with the test compounds; (B) treatment of the cells with the test compounds during post virus infection; (C) treatment of the cells with the test compounds and concurrent infection with the virus. The data is expressed as percent Plaque Forming Unit (PFU) in the compound-treated cells over the untreated virus infected control cells, which were defined as 100%.*Significant at $p < 0.05$ between the viral control and the treated cells.

Open Access Article. Published on 10 September 2020. Downloaded on 1/17/2026 8:55:58 AM.
This article is licensed under a Creative Commons Attribution-NonCommercial 3.0 Unported Licence.

Table 1 Determination of CC_{50}, IC_{50}, and Therapeutic Index (TI) values of **SR-1**, **SR-2**, and Ribavirin[a]

S. no.	Parameter		**SR-1** (μg mL^{-1})	**SR-2** (μg mL^{-1})	Ribavirin (μg mL^{-1})
1	MNCC		62.5*	40*	31.25*
2	CC_{50}		600*	400*	400*
3	Pre-treatment	IC_{50}	10*	20*	40*
		TI	60	20	10
4	Post-treatment	IC_{50}	—	—	—
		TI	—	—	—
5	Simultaneous treatment	IC_{50}	—	30*	—
		TI	—	13.33	—

[a] MNCC – maximum non-cytotoxic concentration; CC_{50} – 50% cytotoxic concentration; IC_{50} – 50% inhibitory concentration; TI – therapeutic index. *Results were obtained from mean ± STD and are significant at $p < 0.05$ between the viral control and the treated cells.

In the third experiment, the compounds were mixed with the virus, incubated at 4 °C for 1 h, and then the mixture was added to the DF-1 cells. **SR-1** and **SR-2** reduced the viral plaques by 21% and 52%, respectively, at their maximum test dose compared to 34% by Ribavirin at MNCC (Fig. 4C). The IC_{50} for **SR-2** was found to be 30 μg mL^{-1} but the IC_{50} values could not be determined for **SR-1** and Ribavirin at the tested doses. The treatment of the cells with a mixture of the test compounds and the virus could have led to the competition between the virus and the test compounds to bind to the host cell receptors, or the test compounds could have altered the structure of either the viral surface antigen or the host receptors, thereby reducing the binding efficiency of the virus to the host cell receptors. Also, it may conceivable that the compounds could inhibit the early stages of viral replication such as endocytosis and uncoating, as reported earlier.[32] The MNCC, CC_{50}, IC_{50}, and TI values of **SR-1**, **SR-2**, and Ribavirin are summarized in Table 1.

3.4. Quantification of viral RNAs

NDV carries a single stranded, non-segmented, and negative-sense RNA coding for six structural proteins, namely, nucleoprotein (NP), phosphoprotein (P), matrix protein (M), fusion protein (F), hemagglutinin neuraminidase (HN), and large protein (L), as well as two non-structural (V and W) proteins.[38] NP encapsulates the viral genomic RNA (gRNA) and anti-genomic complementary RNA (cRNA) to resist the host nucleases and to mediate viral RNA replication and transcription *via* RNA-dependent RNA polymerase.[39] To understand the mechanism(s) of anti-NDV activity, strand-specific quantitative PCR was performed to detect the NP region of NDV gRNA, cRNA, and mRNA in both the NDV-infected and compound-treated DF-1 cells as an indirect measurement of the viral replication and transcription.[27] In **SR-1**, **SR-2**, and Ribavirin-treated cells, the amounts of gRNA, cRNA, and mRNA were significantly reduced when compared with those in the viral control (Fig. 5). Tables S1 and S2† represent the primers and CT values, respectively. Fig. S1–S5† represent the supporting molecular data. The decline in the levels of all the three viral RNAs in comparison with their levels in the NDV-infected DF-1 cells (untreated virus control) clearly indicated that the compounds inhibit both NDV replication and transcription.

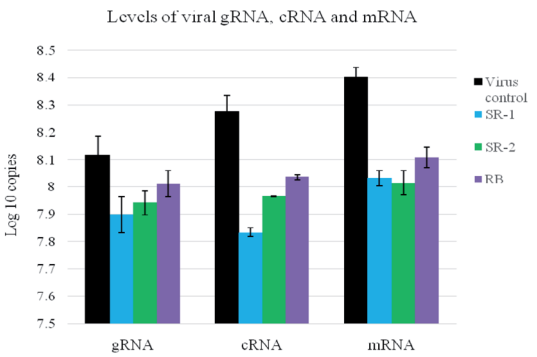

Fig. 5 Effect of compounds **SR-1**, **SR-2**, and Ribavirin (RB) on virus replication and transcription.

3.4.1. Molecular characteristics. In our observations, the viral mRNA content was significantly higher when compared with the gRNA and cRNA levels, which may be due to the degradation of gRNA and cRNA by the host nuclease prior to their encapsidation with the NP protein. NDV replication and transcription depends on the encapsidation of gRNA and cRNA. Therefore, the NP proteins should be preferentially synthesized and the NP gene mRNA transcripts should be abundantly generated at the earliest period of infection.[40] At the mRNA level, both the **SR-1** and **SR-2** treated groups showed a significant reduction when compared with the control but no significant ($p > 0.05$) change was observed between the **SR-1** and **SR-2** treated groups.

A switching mechanism has been proposed in which the viruses regulate the synthesis of different viral RNAs to facilitate infection. For instance, NP, M, and P proteins from influenza A virus, Sendai virus, and measles virus have been reported to play an important role in the switching mechanism between transcription and replication.[41] However, a similar regulation of viral RNA synthesis has not been explored in NDV until now.

The results appear to be in good agreement with similar reports,[42] which show that the cRNA levels were higher and exceeded the amount of gRNA within the infected cells. Also, the rapid accumulation of cRNA *versus* gRNA could be a specific

 This journal is © The Royal Society of Chemistry 2020

Open Access Article. Published on 10 September 2020. Downloaded on 1/17/2026 8:55:58 AM.
This article is licensed under a Creative Commons Attribution-NonCommercial 3.0 Unported Licence.

characteristic of the paramyxovirus, *i.e.*, NDV, which is supported by similarly reported results on the Nipah virus,[43] where the intracellular vRNA of the Nipah virus was much higher than the extracellular vRNA. From the above observations and the results, it is concluded that a paramyxovirus, NDV cRNA, is totally encapsidated by the NP protein that protects cRNA degradation by cellular nucleases. Hence, cRNA is preserved in the cells and accumulates steadily, whereas gRNA undergoes degradation and the amount of progeny cRNA is higher than that of gRNA.

3.5. Docking studies and bioavailability

NDV has two district surface glycoproteins, namely, a hemagglutinin neuraminidase (HN) and a fusion (F) protein. Indeed, HN confers three significant roles: (i) it distinguishes the receptor with sialic acid sites on the cell surfaces; (ii) it enhances the F protein fusion activity and viral penetration ability on the cell surfaces; and (iii) it displays sialidase enzyme activity by removing the sialic acids from the progeny viral particles. However, the HN molecule aids in the designing of novel antiviral drugs using structure-based drug design approach against paramyxovirus diseases.

Therefore, in the present study, the docking experiments of isolated compounds maackiain (**SR-1**) and echinoisoflavonone (**SR-2**) were conducted using the HN protein. As a result, **SR-2** showed greater binding affinity of −8.0 kcal mol^{-1} than that of **SR-1** with −7.6 kcal mol^{-1}. The functional groups present in compound **SR-2** positioned within the sialic acid site of the HN protein, exhibiting foremost interactions with the hotspot residues such as the 2′ and 4′-dimethoxy residues, showed two bonds with Lys236 and Ser237, 3-OH bond with Tyr526, 5-OH group with Arg363, whereas the 7-hydroxy group with Arg416 and the keto group at the 4-position showed two bonding interactions with Glu258 and Tyr317, respectively (Fig. 6a; Table 2). On the other hand, **SR-1** exhibited nine molecular interactions with the certain residues, which include the 3-OH group with Lys236 and one pi–pi interaction with His199, the 5-oxygen group interaction with Ser237, the 11-oxygen atom formed two interactions with Ile175 and Tyr526, the 8-oxygen atom formed interactions with Tyr526 and Arg416, and the 9-oxygen atom displayed two bonded interactions with Tyr317 and Glu258 (Fig. 6b). Furthermore, the physiochemical properties and the toxicity measurements were assessed using Lipinski's rule of five through *in silico* experiments (Table 3). The bioavailability of the isolates was confirmed as the molecular weight was found to be less than 500, H-bond donors were found to be less than five, the H-bond acceptors were found to be less than ten, and the partition coefficient (cLogP) was predicted to be less than five. These *in silico* experiments revealed that both the isolates were non-toxic in terms of mutagenic as well tumorigenic properties and beneficial as antiviral agents for treating viral infections.

Table 2 Bonding interactions, bond distance, and binding energy of **SR-1** and **SR-2** with the HN protein

Comp.	Interactions		Distance (Å)	Binding energy (Δ, kcal mol^{-1})
	Protein	Ligand		
SR-1	His_{199}	3OH	3.1	−7.6
	Lys_{236}	Arene	3.5	
	Ser_{237}	5O	4.4	
	Lys_{235}	Arene	3.5	
	Ile_{175}	11O	3.5	
	Arg_{174}	11O	4.6	
	Tyr_{526}	O	3.8	
	Arg_{416}	O	3.6	
	Glu_{258}	O	4.4	
	Tyr_{317}	O	2.7	
SR-2	Lys_{236}	2′OCH_2	3.6	−8.0
	Ser_{237}	4′OCH_2	4.2	
	Tyr_{526}	3OH	2.8	
	Arg_{174}	4O	5.0	
	Glu_{258}	O	4.7	
	Tyr_{317}	O	2.7	
	Arg_{363}	5OH	4.2	
	Arg_{416}	7OH	4.4	

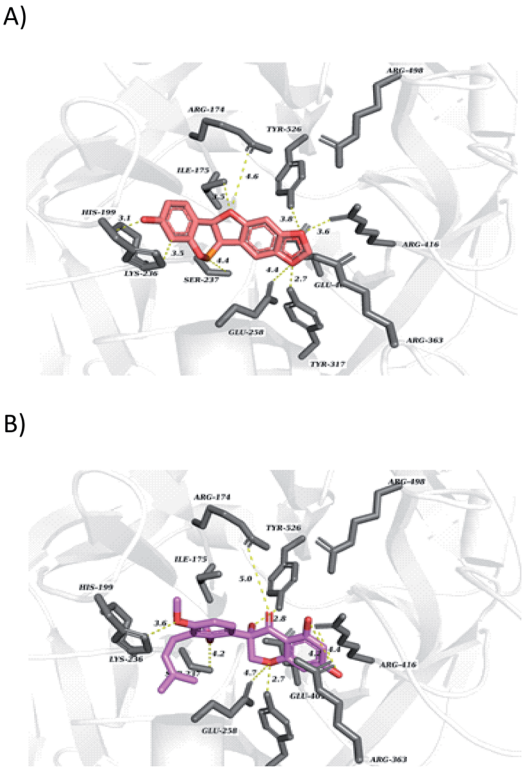

Fig. 6 Binding interactions of the isolates (A) **SR-1** and (B) **SR-2** with the hotspot residues of hemagglutinin neuraminidase (HN) protein. The protein is shown in the white transparent cartoon model and the key residues are depicted in gray50 color with labeling. The molecular interaction network is rendered with dotted lines with bond distances in angstrom.

4. Conclusions

In the current study, we have successfully isolated and characterized two flavonoids, namely, maackiain (**SR-1**) and

Open Access Article. Published on 10 September 2020. Downloaded on 1/17/2026 8:55:58 AM. This article is licensed under a Creative Commons Attribution-NonCommercial 3.0 Unported Licence.

Table 3 Computed physiochemical properties and toxicity measurements using Lipinski's rule of five

Comp.	Physiochemical properties	Drug likeness/toxicity properties
SR-1	Formula: $C_{16}H_{12}O_5$ Mol. weight: 284.26 g mol^{-1} Number of heavy atoms: 21 No. of aromatic heavy atoms: 12 Fraction Csp3: 0.25 Rotatable bonds: 0 H-bond acceptors: 5 H-bond donors: 1 Molar refractivity: 72.74 TPSA ($Å^2$): 57.15	Mutagenic: no Tumorigenic: no Irritant: mild
SR-2	Formula: $C_{22}H_{24}O_7$ Mol. weight: 400.42 g mol^{-1} Number of heavy atoms: 29 No. of aromatic heavy atoms: 12 Fraction Csp3: 0.32 Rotatable bonds: 5 H-bond acceptors: 7 H-bond donors: 3 Molar refractivity: 107.30 TPSA ($Å^2$): 105.45	Mutagenic: no Tumorigenic: no Irritant: no

echinoisoflavanone (**SR-2**), from *Sophora interrupta* Bedd. root extract and their antiviral properties as well as their molecular mechanisms were evaluated. The results showed that both the isolated compounds have comparatively good *in vitro* antiviral activities than the standard antiviral drug, Ribavirin. In particular, compound **SR-2** was found to be more potent than maackiain and Ribavirin against NDV *in vitro*. Also, these compounds inhibit viral adsorption, replication, and transcription, thus demonstrating their potential therapeutic effects not only in birds but also against other paramyxoviruses that infect humans and animals. Further efforts for exploring their *in vivo* antiviral activity and their pharmacokinetics are underway, which will aid in developing them as potential antiviral drugs.

Conflicts of interest

There are no conflicts to declare.

Acknowledgements

The author WR thanks the Council of Scientific and Industrial Research (CSIR), New Delhi and the authors CB, AR, and PR are grateful to UGC-BSR, New Delhi for financial assistance under CSIR-MRP and UGC-RFSMS (BSR) programs. Furthermore, all the authors are thankful to National Institute of Animal Biotechnology (NIAB), Hyderabad for providing laboratory facilities to carry out the viral studies.

References

1 D. J. Alexander and D. A. Senne, Newcastle disease, other avian paramyxoviruses, and pneumovirus infections, in *Diseases of Poultry*, ed. Y. M. Saif, A. M. Fadly, J. R. Glisson, L. R. McDougald, L. K. Nolan and D. E. Swayne, Blackwell Publishing, Lova, USA, 12th edn, 2008, pp. 75–115.
2 L. Dufour-Zavala, *A laboratory manual for the isolation, identification, and characterization of avian pathogens*, American Association of Avian Pathologists, Jacksonville, Fl., USA, 5th edn, 2008, pp. 135–141.
3 D. J. Alexander and R. E. Gough, Newcastle disease, other avian Paramyxoviruses, and Pneumovirus infections, in *Disease of Poultry*, ed. Y. M. Saif, H. J. Barnes, J. R. Glisson, A. M. Fadly, L. R. McDougald, L. K. Nolan, D. E. Swayne, Iowa State Press, Ames, IA 1A, 11th edn, 2003, pp. 63–99.
4 G. Elia, C. Belloli, F. Cirone, M. S. Lucente, M. Caruso, V. Martella, N. Decaro, C. Buonavoglia and P. Ormas, *Antiviral Res.*, 2008, **77**(2), 108–113.
5 B. E. Gilbert and V. E. Knight, *Antimicrob. Agents Chemother.*, 1986, **30**(2), 201.
6 N. J. Snell, *Expert Opin. Pharmacother.*, 2001, **2**, 1317–1324.
7 J. Fackler, K. Flannery, M. Zipkin and K. McIntosh, *N. Engl. J. Med.*, 1990, **322**(9), 634.
8 M. F. Hebert and B. J. Guglielmo, *Dicp*, 1990, **24**(7–8), 735–738.
9 S. A. Jassim and M. A. Naji, *J. Appl. Microbiol.*, 2003, **95**(3), 412–427.
10 J. Yasuhara-Bell and Y. Lu, *Antiviral Res.*, 2010, **86**(3), 231–240.
11 A. Raza, F. Muhammad, S. Bashir, M. I. Anwar, M. M. Awais, M. Akhtar, B. Aslam, T. Khaliq and M. U. Naseer, *World's Poult. Sci. J.*, 2015, **71**(3), 523–532.
12 T. M. Babu, S. S. Rajesh, B. V. Bhaskar, S. Devi, A. Rammohan, T. Sivaraman and W. Rajendra, *RSC Adv.*, 2017, **7**(30), 18277–18292.
13 T. Lane, M. Anantpadma, J. S. Freundlich, R. A. Davey, P. B. Madrid and S. Ekins, *Pharm. Res.*, 2019, **36**(7), 104.
14 M. H. Oak, C. Auger, E. Belcastro, S. H. Park, H. H. Lee and V. B. Schini-Kerth, *Free Radical Biol. Med.*, 2018, **122**, 161–170.
15 J. S. Gamble, *Flora of the presidency of madras*, London, Adlard & Son, 1935, vol. 1, p. 389.
16 Z. H. Zheng, Z. H. Dong and J. She, *Modern studies on traditional Chinese medicine*, Xue Yuan Press, Beijing, 1st edn, 1997.
17 Y. Zhang, H. Zhu, G. Ye, C. Huang, Y. Yang, R. Chen, Y. Yu and X. Cui, *Life Sci.*, 2006, **78**(17), 1998–2005.
18 K. Kitazato, Y. Wang and N. Kobayashi, *Drug Discoveries Ther.*, 2007, **1**(1), 14–22.
19 P. M. Krishna and K. N. V. Rao, *Rev. Bras. Farmacogn.*, 2012, **22**(5), 1145–1154.
20 J. F. Yang, C. H. Yang, C. C. Wu and L. Y. Chuang, *J. Pharmacogn. Phytochem.*, 2015, **3**(6), 26–31.
21 R. Munikishore, A. Rammohan, A. Padmaja, D. Gunasekar, A. Deville and B. Bodo, *Nat. Prod. Res.*, 2013, **27**(20), 1823–1826.
22 A. Rammohan, R. Munikishore, D. Gunasekar, A. Deville and B. Bodo, *Nat. Prod. Res.*, 2015, **29**(1), 82–85.
23 C. Bhuvaneswar, P. Rames, C. Venkataramaiah, G. Sandeep and W. Rajendra, *Int. J. Phytomed.*, 2017, **9**, 426–435.

 This journal is © The Royal Society of Chemistry 2020

Open Access Article. Published on 10 September 2020. Downloaded on 1/17/2026 8:55:58 AM.
This article is licensed under a Creative Commons Attribution-NonCommercial 3.0 Unported Licence.

24 J. Parekh and S. Chanda, *Afr. J. Biomed. Res.*, 2006, **9**(2), 89–93.
25 U. P. Singh, B. K. Sarma, D. P. Singh and A. Bahadur, *Curr. Microbiol.*, 2002, **44**(6), 396–400.
26 T. Mosmann, *J. Immunol. Methods*, 1983, **65**(1–2), 55–63.
27 X. Qiu, Y. Yu, S. Yu, Y. Zhan, N. Wei, C. Song, Y. Sun, L. Tan and C. Ding, *Sci. World J.*, 2014, **2014**, 1–10.
28 S. Crennell, T. Takimoto, A. Portner and G. Taylor, *Nat. Struct. Biol.*, 2007, **11**, 1068–1074.
29 O. Trott and A. J. Olson, *J. Comput. Chem.*, 2010, **31**(2), 455–461.
30 R. Huey, G. M. Morris, A. J. Olson and D. S. Goodsell, *J. Comput. Chem.*, 2007, **28**(6), 1145–1152.
31 W. L. DeLano, *CCP4 Newsletter on protein crystallography*, 2002, **40**(1), 82–92.
32 C. H. Chao, Q. I. Jian-bin, M. A. Da-you, S. H. Na and H. U. Chang-qi, *Nat. Prod. Res. Dev.*, 2008, **20**(3), 472–473.
33 C. J. Xiao, Y. Zhang, L. Qiu, X. Dong and B. Jiang, *Planta Med.*, 2014, **80**(18), 1727–1731.
34 C. M. KIim, Y. Ebizuka and U. Sankawa, *Chem. Pharm. Bull.*, 1989, **37**(10), 2879–2881.
35 R. Elizondo-Gonzalez, L. E. Cruz-Suarez, D. Ricque-Marie, E. Mendoza-Gamboa, C. Rodriguez-Padilla and L. M. Trejo-Avila, *Virol. J.*, 2012, **9**(1), 307.
36 Z. Yang, Y. Wang, Z. Zheng, S. Zhao, J. I. Zhao, Q. Lin, C. Li, Q. Zhu and N. Zhong, *Int. J. Mol. Med.*, 2013, **31**(4), 867–873.
37 D. G. Streeter, J. T. Witkowski, G. P. Khare, R. W. Sidwell, R. J. Bauer, R. K. Robins and L. N. Simon, *Proc. Natl. Acad. Sci. U. S. A.*, 1973, **70**(4), 1174–1178.
38 R. A. Lamb and D. Kolakofsky, *Paramyxoviridae: the viruses and their replication*, Lippincott Williams & Wilkins, Hagerstown, 4th edn, 2001.
39 S. I. Vidal and D. A. Kolakofsky, *J. Virol.*, 1989, **63**(5), 1951–1958.
40 B. P. H. Peeters, Y. K. Gruijthuijsen, O. S. De Leeuw and A. L. J. Gielkens, *Arch. Virol.*, 2000, **145**(9), 1829–1845.
41 A. DiCarlo, B. Nadine, H. Bettina, K. Anja and B. Stephan, *J. Infect. Dis.*, 2011, **204**(3), 927–933.
42 X. Qiu, Y. Yu, S. Yu, Y. Zhan, N. Wei, C. Song, Y. Sun, L. Tan and C. Ding, *Sci. World J.*, 2014, **2014**, 1–10.
43 L. Y. Chang, A. M. Ali, S. S. Hassan and S. AbuBakar, *Virol. J.*, 2006, **3**(1), 47.